

PCCP

Accepted Manuscript



This is an *Accepted Manuscript*, which has been through the Royal Society of Chemistry peer review process and has been accepted for publication.

Accepted Manuscripts are published online shortly after acceptance, before technical editing, formatting and proof reading. Using this free service, authors can make their results available to the community, in citable form, before we publish the edited article. We will replace this *Accepted Manuscript* with the edited and formatted *Advance Article* as soon as it is available.

You can find more information about *Accepted Manuscripts* in the [Information for Authors](#).

Please note that technical editing may introduce minor changes to the text and/or graphics, which may alter content. The journal's standard [Terms & Conditions](#) and the [Ethical guidelines](#) still apply. In no event shall the Royal Society of Chemistry be held responsible for any errors or omissions in this *Accepted Manuscript* or any consequences arising from the use of any information it contains.

This manuscript has been authored by UT-Battelle, LLC under Contract No. DE-AC05-00OR22725 with the U.S. Department of Energy. The United States Government retains and the publisher, by accepting the article for publication, acknowledges that the United States Government retains a non-exclusive, paid-up, irrevocable, world-wide license to publish or re-

produce the published form of this manuscript, or allow others to do so, for United States Government purposes. The Department of Energy will provide public access to these results of federally sponsored research in accordance with the DOE Public Access Plan (<http://energy.gov/downloads/doe-public-access-plan>).

Predictive Modeling of Synergistic Effects in Nanoscale Ion Track Formation

Eva Zarkadoula,¹ Olli H. Pakarinen,^{1,2} Haizhou Xue,³ Yanwen Zhang,¹ and William J. Weber^{3,1}

¹*Materials Science & Technology Division, Oak Ridge National Laboratory, Oak Ridge, TN 37831, USA**

²*Department of Physics, University of Helsinki, P.O. Box 64, FI-00014, Finland*

³*Department of Materials Science & Engineering, University of Tennessee, Knoxville, TN 37996, USA*

Molecular dynamics techniques in combination with the inelastic thermal spike model are used to study the coupled effects of the inelastic energy loss due to 21 MeV Ni ion irradiation with pre-existing defects in SrTiO₃. We determine the dependence on pre-existing defect concentration of nanoscale track formation occurring from the synergy between the inelastic energy loss and the pre-existing atomic defects. We show that the size of nanoscale ion tracks can be controlled by the concentration of pre-existing disorder. This work identifies a major gap in fundamental understanding on the role of defects in electronic energy dissipation and electron-lattice coupling.

Ion irradiation of materials has been finding increasing applications in various fields with notable examples of semiconductor and nuclear industries, in ion beam modification of materials and material characterization. During irradiation, highly energetic ions lose part of their energy to the nuclei of the target material (elastic energy loss) and the remaining energy in interactions with the electrons (inelastic energy loss). Although it is well known that the elastic energy loss results in the creation of point defects and defect clusters, the effects of the inelastic energy loss on the defect production¹⁻³ and damage evolution are not well understood^{4,5}.

Recent studies have emphasized the importance of the effects of the coupling of electronic and atomic processes in ionic and covalent materials¹⁻¹⁴, and have shown that these effects can have linearly additive¹⁻⁶ or competing⁷⁻⁹ impacts on the defect production. However, ionization processes^{10,11} and nonlinear combination of electronic and nuclear energy loss^{3,12} result in more complex behavior. A remarkable synergy between inelastic energy loss and pre-existing point defects is demonstrated in recently published experimental results¹⁵, where it is shown that no ion tracks are created during 21 MeV Ni ion irradiation of crystalline SrTiO₃, but amorphous tracks are produced in pre-damaged samples. Molecular dynamics (MD) modeling results included in the latter study confirm the synergy of the electronic energy loss with the atomic defects in the creation of the ion tracks, while a more recent MD study shows a temperature dependence and electronic energy loss dependence of the ion track size in pre-damaged SrTiO₃ systems¹⁶. In the present study, we use MD simulations to study the effects of defect concentration on the size and morphology of nanoscale amorphous ion tracks in cubic pre-damaged SrTiO₃.

SrTiO₃ is a wide band-gap perovskite-type oxide widely studied for micro- and opto- electronics¹⁷⁻²² and nuclear applications²³. SrTiO₃ thin films can be used as a ferroelectric²⁴ and as a high temperature superconductor²⁵. Recently discovered magnetic properties of SrTiO₃ describe it as a critical material in the functional oxide electronics area²⁶, while metallic interfaces in amorphous SrTiO₃-based heterostructures show conducting behavior²⁷ similar to transparent conducting layers of SrTiO₃ produced by 300 eV Ar irradiation²⁸.

We use an inelastic Thermal Spike (ITS) model suitable for insulators²⁹ to include the electronic energy loss effects in the simulations. In this model, the atomic and the electronic subsystems are coupled and the energy exchange between them is described via a set of heat diffusion equations, one describing the evolution of the electronic temperature, T_e (1), and one describing the evolution of the atomic temperature, T_a (2).

$$C_e \frac{\partial T_e}{\partial t} = \frac{1}{r} \frac{\partial}{\partial r} \left[r K_e \frac{\partial T_e}{\partial r} \right] - g(T_e - T_a) + A(r, t) \quad (1)$$

$$C_a \frac{\partial T_a}{\partial t} = \frac{1}{r} \frac{\partial}{\partial r} \left[r K_a \frac{\partial T_a}{\partial r} \right] + g(T_e - T_a) \quad (2)$$

The hot electrons transfer energy to the lattice via the electron-phonon interactions. The second term on the right side of the equations (1) and (2) represents the energy exchange between the electronic and atomic subsystems due to the difference between T_e and T_a . C_e and C_a are the specific heat coefficients of the electronic and atomic systems respectively, whereas K_e and K_a are the thermal conductivities of the electronic and the atomic systems. The term g is the electron-phonon coupling pa-

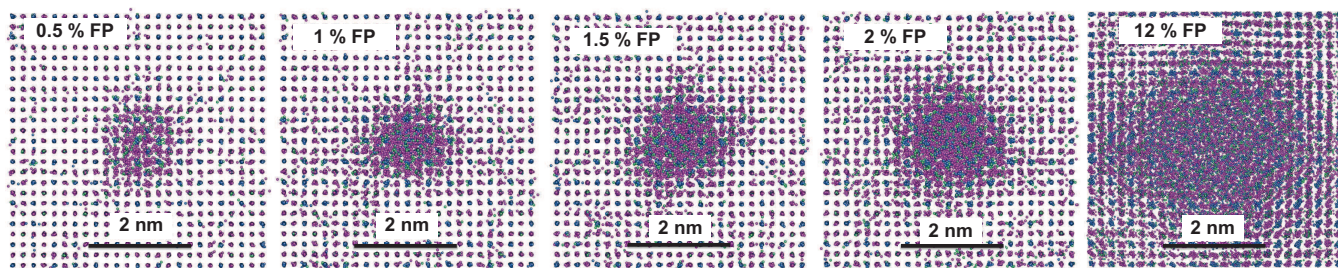


FIG. 1: Cross sections of five pre-damaged systems with different initial defect concentration along the [001] direction, after a thermal spike of 21 MeV Ni ions. Sr is shown in blue, Ti in green, and O in purple.

parameter, and $A(r, t)$ describes the energy deposition from the incident ion to the electrons³⁰.

We used $C_e = 1 \text{ J cm}^{-3} \text{ K}^{-129,31,32}$ and $C_a = 0.544 \text{ J g}^{-1} \text{ K}^{-133}$ for the electronic and the atomic systems, respectively. Irradiation-induced defects are known to scatter phonons and electrons resulting in significant decrease in the thermal conductivity of irradiated ceramics^{34,35}; therefore, we used reduced values of both K_e and K_a by an order of magnitude in comparison to the values for the perfect crystalline system. Such a decrease in the thermal conductivity is reasonably consistent with the large changes in thermal conductivity of SrTiO_3 due to processing defects³⁶ or cation non-stoichiometry (a few percent)³⁷. For the crystalline system K_e is equal to $K_e = C_e D_e$, where D_e is the thermal diffusivity, as previously suggested^{29,31,32}, while K_a is equal to $11.2 \text{ W m}^{-1} \text{ K}^{-1}$ at 300 K. The value of g for a crystalline system is, as described elsewhere²⁹, $4.3 \times 10^{18} \text{ W m}^{-3} \text{ K}^{-1}$. We used a 35% larger value for the pre-damaged system to account for the decrease in the electron-phonon mean free path due to defects. The electronic energy loss due to 21 MeV Ni ions at about 120 nm depth is calculated with Stopping and Range of Ions in Matter (SRIM) code³⁸ to be about 9.74 keV/nm. The calculated energy deposition is then used as input in the MD simulations.

We use the DL.POLY³⁹ MD simulation package to simulate 21 MeV Ni ion irradiation and pre-damaged systems consisting of about 7 million atoms. We use empirical potentials by McCoy et al.⁴⁰ joined to the ZBL⁴¹ repulsive potentials for short distances. The ZBL potential was used for all pair interactions. The pre-damaged systems were created by introducing stoichiometric Frenkel pairs (FP) of all three atomic species randomly in the systems. Subsequently all systems were relaxed under constant pressure and temperature.

The irradiation of the systems was along the z direction under the constant-energy, constant-volume (NVE) ensemble at 300 K, with a variable timestep, in a total depth of about 260 Å. The atoms contained in the x and y boundary of the MD box, in a layer of about 10 Å thickness, are connected to a langevin thermostat at 300 K to emulate the effect of energy dissipation into the sample. The defects are identified using the sphere

criterion⁴², with a cut-off radius of 0.75 Å.

We ran a total of six MD simulations: we applied the iTS in five pre-damaged systems, with different disorder level, and we ran one more simulation in a system where FP are contained only in half the MD box, while the other half is crystalline, free of FP. Previous MD simulations for 21 MeV Ni ions in a perfect crystalline structure¹⁵, with iTS parameters for the perfect crystal, showed clearly no defects or track formation.

Figure 1 shows cross sections of systems with different pre-existing defects, of 0.5% to 12% FP concentration. The ion track diameter depends on the level of the pre-existing disorder in the system and it increases for increased disorder. Figure 2 shows slices in the xz-plane of the five pre-damaged systems shown in Fig. 1. In this figure we see that the ion track becomes more continuous as the defect density increases. The non-continuous morphology seen in low disorder level systems, as well as variations of the track diameter size along the ion track in systems with larger disorder level, can be attributed to the inhomogeneity of the defect distribution along the ion path. The ion track diameter ranges from approximately $1.2 \text{ nm} \pm 0.17 \text{ nm}$ to about $2.6 \text{ nm} \pm 0.61 \text{ nm}$.

A linear dependence of ion track diameter on Frenkel pair concentration from the MD simulations is shown in Figure 3 (a). Track diameters determined experimentally for pre-damaged SrTiO_3 irradiated with 21 MeV Ni ions exhibit a similar linear dependence on measured disorder, as shown in Figure 3 (b). The experimental track diameters for disorder levels at or below 7% were reported previously¹⁵ and the track diameter at the higher disorder level (11%) was determined using identical procedures¹⁵ but in a sample with a higher level of initial disorder. As seen here similar trends suggest a good agreement between the computational and experimental results, and both indicate a linear relationship between average track diameter and initial pre-damage level. The discrepancy in slope is because we did not change any of the two-temperature model parameters in the simulations with increasing disorder, as such a variation would be premature until a more exact measurement of defect concentration is possible. Additionally, we note that the percentage of the FP in the MD simulations is

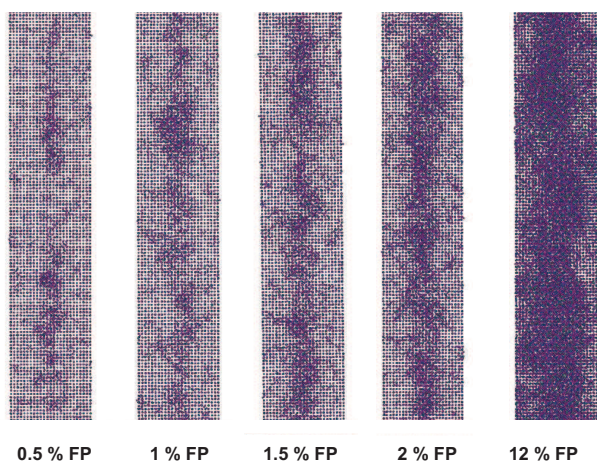


FIG. 2: Perpendicular slices of the configuration of the pre-damaged samples and 21 MeV Ni ion tracks shown in Fig. 1. Sr is shown in blue, Ti in green, and O in purple.

not equivalent to the percentage of disorder measured by ion channeling⁴³, since the disorder observed along a channel may only be a fraction of the actual defect concentration⁴⁴.

These results show a significant synergy occurring between the inelastic energy loss and pre-existing atomic defects. The phonons are scattered while passing through the defected region, resulting in a reduced energy flow which is expressed as decreased thermal conductivity⁴⁵. Additionally, the role of the defects as scattering centers results in decrease of the electron-lattice relaxation time $\tau = C_e/g$, which is related to the electron-lattice interaction mean free path λ by $\lambda^2 = D_e\tau$. With the thermal conductivity of the electrons K_e linked to the thermal diffusivity by $K_e = D_e C_e$, the reduced electron-lattice interaction mean free path λ results in stronger electron-phonon coupling $g = K_e/\lambda^{229}$. In combination with the fact that the relaxation time between collisions is proportional to $1/N_c$, where N_c is the number of scattering centers, the above effects mean that the increased disorder affects the heat transfer and consequently the energy dissipation in the system. Furthermore, the pre-existing defects and defect clusters in the vicinity of the ion path are subject to extreme heating and can act as nucleation centers accumulating the disorder along the ion path.

The crucial presence of defects in the simulation cell is

also demonstrated in Figure 4 where we show a system half crystalline and half pre-damaged. Figure 4 shows a perpendicular slice of the final configuration of this system, where an ion track is created only in the pre-damaged region (0.5 % FP in the upper half), while there are only a few defects created in the crystalline region. In the pre-damaged region the energy transferred from the electronic to the atomic system, including the existing defects, increases the disorder in the vicinity of the ion path resulting in ion track formation. In the crystalline region the deposited energy is not sufficient to amorphize the material and we observe elastic recovery of almost all the damaged induced. The role of the pre-existing disorder is paramount, as ion tracks will not necessarily form in any system that exhibits similar values of decreased thermal conductivity and increased e-ph phonon coupling as the ones used here.

In summary, our results demonstrate that the synergy between atomic defects and the inelastic energy loss results in the formation of nanometer-sized ion tracks only in systems with pre-existing disorder and they show linear dependence of the ion track size on the pre-existing damage level. The pre-existing damage affects the way the energy is dissipated from the electronic to the atomic system, and plays a crucial role in the ion track size and morphology. The presence of the defects results in reduced thermal conductivity and stronger e-ph coupling, and the local heating increases the disorder near the ion path, affecting the ion track size and shape. The MD results show that higher disorder level in the system results in larger and more continuous ion tracks, in agreement with experimental findings. This work identifies a major gap in fundamental understanding on the role of defects in electronic energy dissipation and electron-lattice coupling. It also provides new insights for creating novel interfaces and nanostructures to functionalize thin-film structures, including tunable electronic, magnetic and optical properties. Further investigation of the coupled effects of inelastic energy loss and pre-existing defects is needed in order to understand fundamental aspects of irradiation effects in materials and predict their performance.

This work was supported by the U.S. Department of Energy, Office of Science, Basic Energy Sciences, Materials Sciences and Engineering Division. This research used resources of the National Energy Research Scientific Computing Center, supported by the Office of Science, US Department of Energy under Contract No. DEAC02-05CH11231.

* Electronic address: zarkadoulae@ornl.gov

¹ M. Toulemonde, W. j. Weber, G. Li, V. Shutthanandan, P. Kluth, T. Yang, Y. Wang, Y. Zhang, *Phys. Rev. B*, 2011, **83**, 054106.

² L. Thom e, A. Debelle, F. Garrido, P. Trocellier, Y. Serruys,

G. Velisa, S. Miro, *Appl. Phys. Lett.*, 2013, **102**, 141906.

³ M. Sall, I. Monnet, C. Grygiel, B. Ban dEtat, H. Lebius, S. Leclerc, E. Balanzat, *EPL*, 2013, **102**, 26002.

⁴ . Zhang, D. S. Aidhy, T. Varga, S. Moll, P. D. Edmondson, F. Namavar, K. Jin, C. N. Ostrouchov, W. J. Weber, *Phys.*

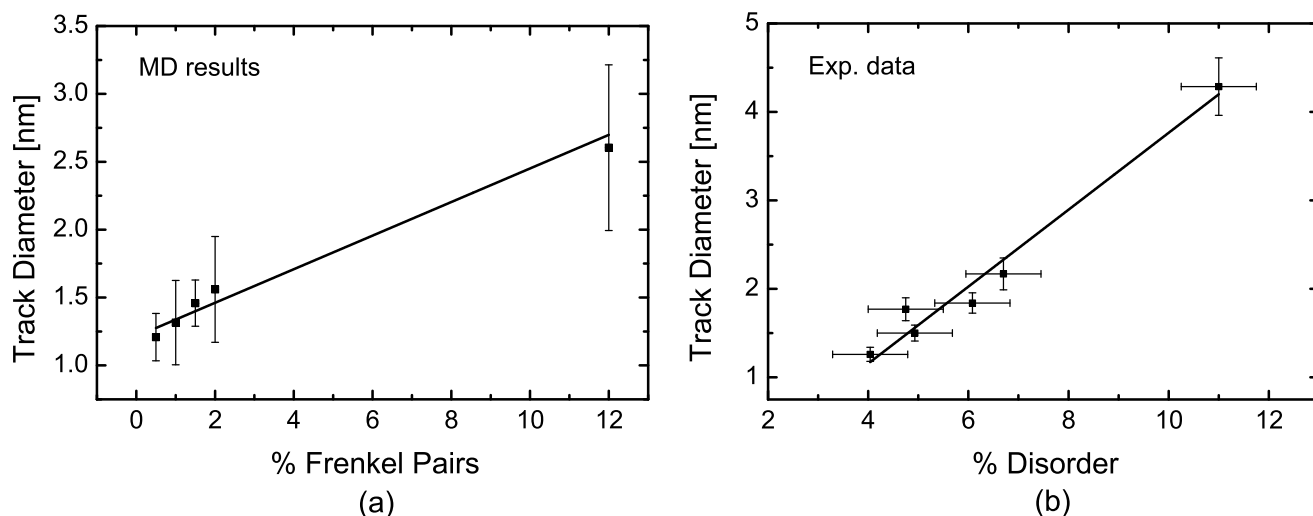


FIG. 3: Ion track diameter for 21 MeV Ni ions as a function of initial different disorder level. (a) MD results are plotted as a function of FP concentration. The error bars represent the standard deviation over different measurements of the diameter along the ion tracks. (b) Experimental results as a function of the disorder percentage (the error bars are discussed in Ref.¹⁵). The fit for both data sets is plotted and indicates a linear relationship between the track diameter and the initial disorder level.

Chem. Chem. Phys., 2014, **16**, 8051-8059.

- ⁵ Y. Y. Wang, C. Grygiel, C. Dufour, J. R. Sun, Z. G. Wang, Y. T. Zhao, G. Q. Xiao, R. Cheng, X. M. Zhou, J. R. Ren, S. D. Liu, Y. Lei, Y. B. Sun, R. Ritter, E. Gruber, A. Cas-simi, I. Monnet, S. Bouffard, F. Aumayr, M. Toulemonde, *Sci. Rep.*, 2014, **4**, 5742.
- ⁶ M. Backman, F. Djurabekova, O. H. Pakarinen, K. Nordlund, Y. Zhang, M. Toulemonde, W. J. Weber *J. Phys. D: Appl. Phys.*, 2012, **45**, 505305.
- ⁷ A. Debelle, M. Backman, L. Thomé, W. J. Weber, M. Toulemonde, S. Mylonas, A. Boulle, O. H. Pakarinen, N. Juslin, F. Djurabekova, K. Nordlund, F. Garrido, D. Chaussende *Phys. Rev. B*, 2012, **86**, 100102.
- ⁸ W. J. Weber, Y. Zhang, H. Y. Xiao, L. M. Wang, *RSC Advances*, 2012, **2**, 595-604.
- ⁹ Y. Zhang, T. Varga, M. Ishimaru, P.D. Edmondson, H. Xue, P. Liu, S. Moll, F. Namavar, C. Hardiman, S. Shannon, W. J. Weber *Nucl. Instrum. Methods. Phys. Res. B*, 2014, **327**, 33-43.
- ¹⁰ S. J. Zinkle, V. Skuratov, D. T. Hoelzer, *Nucl. Instrum. Methods Phys. Res. B*, 2002, **191**, 758-766.
- ¹¹ C. Kinoshita, K. Yasuda, S. Matsumura, M. Shimada, *Metall. Mater. Trans. A*, 2004, **35**, 2257-2266.
- ¹² A. Kamarou, W. Wesch, E. Wendler, *Phys. Rev. B*, 2008, **78**, 054111.
- ¹³ D. M. Duffy, S. L. Daraszewicz, J. Mulroue, *Nucl. Instrum. Methods Phys. Res. B*, 2012, **277**, 21-27.
- ¹⁴ W. J. Weber, D. M. Duffy, L. Thomé, Y. Zhang, *Curr. Opin. Solid State Mater. Sci.*, 2015, **19**, 1-11.
- ¹⁵ W. J. Weber, E. Zarkadoula, O. H. Pakarinen, R. Sachan, M. F. Chisholm, P. Liu, H. Xue, K. Jin, Y. Zhang, *Sci. Rep.*, 2015, **5**, 7726.
- ¹⁶ E. Zarkadoula, O. H. Pakarinen, H. Xue, Y. Zhang, W. J. Weber *Scripta Mater.*, 2015, doi:10.1016/j.scriptamat.2015.05.044
- ¹⁷ K. Oyoshi, S. Hishita, H. Haneda, *J. Appl. Phys.*, 2000, **87**, 3450-3456.
- ¹⁸ G. D. Wilk, R. M. Wallace, J. M. Anthony, *J. Appl. Phys.*, 2001, **89**, 5243-5275.
- ¹⁹ N. Erdman, K.R. Poeppelmeler, M. Asta, O. Warschkow, D.E. Ellis, L.D. Marks, *Nature*, 2002, **419**, 55.
- ²⁰ A. Kosola, M. Putkonen, L. S. Johansson, L. Niinist, *Appl. Surf. Sci.*, 2003, **211**, 102-112.
- ²¹ J. H. Haeni, P. Irvin, W. Chang, R. Uecker, P. Reiche, Y. L. Li, S. Choudhury, W. Tian, M. E. Hawley, B. Craigo, A. K. Tagantsev, X. Q. Pan, S. K. Streiffer, L. Q. Chen, S. W. Kirchoefer, J. Levy, D. G. Schlom, *Nature*, 2004, **430**, 758-761.
- ²² A. Spinelli, M. A. Torija, C. Liu, c. Jan, C. Leighton, *Phys. Rev. B*, 2010, **81**, 1555110.
- ²³ W. J. Weber, R. C. Ewing, R. C. A. Catlow, T. Diaz de la Rubia, L. W. Hobbs, C. Kinoshita, H. Matzke, A. T. Motta, M. Nastasi, E. K. H. Salje, E. R. Vance, S. J. Zinkle, *Mater. Res.*, 1998, **13**, 1434.
- ²⁴ M. Takesada, M. Itoh, T. Yagi, *Phys. Rev. Lett.*, 2006, **96**, 227602.
- ²⁵ C. S. Koonce, M. H. Cohen, J. F. Schooley, W. E. Hosler, E. R. Pfeiffer *Phys. Rev.*, 1967, **163**, 380.
- ²⁶ W. D. Rice, P. Ambwani, M. Bombeck, J. D. Thompson, G. Haugstad C. Leighton, S. A. Crooker, *Nature Materials*, 2014, **13**, 481-487.
- ²⁷ Y. Chen, N. Pryds, J. E. Kleibeuker, G. Koster, J. Sun, E. Stamate, B. Shen, G. Rijnders, S. Linderorth, *Nano Lett.*, 2011, **11**, 3774-3778.
- ²⁸ D. W. Reagor, V. Y. Butko, *Nature Materials*, 2005, **4**, 593-596.
- ²⁹ M. Toulemonde, W. Assman, C. Dufour, A. Meftah, F. Studer, C. Trautmann, *Mat. Fys. Medd. K. Dan. Vidensk. Selsk.*, 2006, **52**, 263-292.
- ³⁰ M. P. R. Waligorski, R. N. Hamm, R. Katz, *Nucl. Tracks Radiat. Meas.*, 1986, **11**, 309-319.
- ³¹ M. Toulemonde, J. M. Costantini, C. Dufour, A. Meftah,

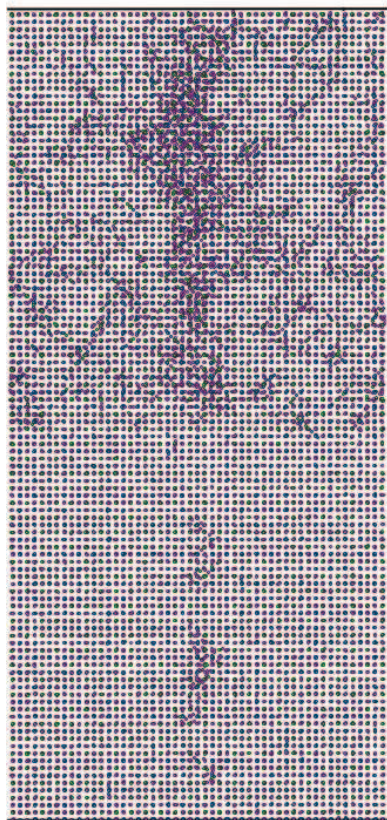


FIG. 4: Perpendicular slice of the final configuration (end of simulation time) for a system which is half pre-damaged (0.5 % FP in the upper half) and half crystalline (lower half). Sr is shown in blue, Ti in green, and O in purple.

- E. Paumier, F. Studer *Nucl. Instr. Meth B*, 1996, **116**, 37.
- 32 A. Meftah, J. M. Costantini, N. Khalfaoui, S. Boudjadar, J. P. Stoquert, F. Studer, M. Toulemonde, *Nucl. Instrum. Methods Phys. Res. B*, 2005, **237**, 563-574.
- 33 Toplent Photonics <http://www.toplent.com/SrTiO3.htm> (accessed March 24, 2015)
- 34 L. L. Snead, S. J. Zinkle, D. P. White, *J. Nucl. Mater.*, 2005, **340**, 187-202.
- 35 P. B. Weisensee, J. P. Feser, D. G. Cahill, *J. Nucl. Mater.*, 2013, **443**, 212-217.
- 36 D-W. Oh, J. Ravichandran, C-W. Liang, W. Siemons, B. Jalan, C. M. Brooks, M. Huijben, D. G. Schlom, S. Stemmer, L. W. Martin, A. Majumdar, R. Ramesh, D. G. Cahill, *Appl. Phys. Lett.*, 2011, **98**, 221904.
- 37 E. Breckenfeld, R. Wilson, J. Karthik, A. R. Damodaran, D. G. Cahill, L. W. Martin, *Chem. Mater.*, 2012, **24**, 331-337.
- 38 J. F. Ziegler, J. P. Biersack and M. D. Ziegler, *SRIM - The Stopping and Range of Ions in Matter.*; SRIM Co.: Chester, MD, USA, 2008.
- 39 I. T. Todorov, B. Smith, M. T. Dove, K. Trachenko, *J. Mater. Chem.*, 2006, **16**, 1911.
- 40 M. A. McCoy, R. W. Grimes, W. E. Lee, *Philos. Mag. A*, 1997, **75**, 833-846.
- 41 J. F. Ziegler, J. P. Biersack, U. Littmark, *The Stopping and Range of Ions in Matter*; Pergamon: New York, 1985.
- 42 I.T. Todorov and W. Smith, *THE DL POLY 4 USER MANUAL*, v.4 2012, www.ccp5.ac.uk/DL_POLY/MANUALS/USRMAN4.pdf
- 43 Y. Zhang, Z. Zhu, W. D. Bennett, L. V Saraf, J.L. Rausch, C. A. Hendricks, W. J. Weber, J. Lian, R. C. Ewing, *J. Nucl. Mater.*, 2009, **389**, 303-310.
- 44 Y. Zhang, F. Gao, W. Jiang, D. E. McCready, W. J. Weber, *Phys. Rev. B*, 2004, **70**, 125203.
- 45 C. P. Flynn, *Point defects and diffusion*; Clarendon Press: Oxford, 1972.